CrossMark

ORIGINAL PAPER

Fractional nuclear charge approach to isolated anion densities for Hirshfeld partitioning methods

Farnaz Heidar-Zadeh[1,2,3] · Paul W. Ayers[3] (iD) · Patrick Bultinck[1]

Abstract Atoms in molecules methods that rely on reference promolecular densities typically require that one define, or otherwise determine, the densities of unbound atomic anions. Whereas the isolated atomic polyanions are always physically and computationally unbound, monoanions can be either physically bound but computationally unbound (like the oxygen anion at the Hartree-Fock level of theory), or physically unbound but computationally bound (like the nitrogen anion using many DFT methods with a basis set including diffuse functions). Depending on the level of theory and basis set used, the densities of negatively charged atomic ions can decay very slowly and even be nonmonotonically decreasing. These delocalized anionic densities induce ill-behaved atomic properties for compounds containing highly reduced atoms. To treat the problem of unphysical proatom densities in iterative Hirshfeld methods, we compute the smallest (typically fractional) nuclear charge to bind all electrons, called the effective nuclear charge Z_A^{eff} of an atom A.

When $Z_A^{eff} > Z_A$ at a given level of theory, the scaled density corresponding to the effective nuclear charge is used as the negatively charged proatom density. This novel approach dramatically improves the computational robustness of the iterative Hirshfeld partitioning scheme.

✉ Paul W. Ayers
  ayers@mcmaster.ca; ayers@chemistry.mcmaster.ca

✉ Patrick Bultinck
  patrick.bultinck@ugent.be

[1] Department of Chemistry, Ghent University, Krijgslaan 281 (S3), 9000 Ghent, Belgium

[2] Center for Molecular Modeling, Ghent University, Technologiepark 903, 9052 Zwijnaarde, Belgium

[3] Department of Chemistry and Chemical Biology, McMaster University, Hamilton, ON L8S 4M1, Canada

Introduction

Methods for identifying the atoms in a molecule (AIM) can be broadly classified based on whether they partition the molecule's wave-function in Hilbert space or divide a molecular descriptor in real space [1]. The latter commonly use the molecular electron density to directly define an AIM density $\rho_A(\mathbf{r})$ by,

$$\rho_A(\mathbf{r}) = w_A(\mathbf{r})\rho_{mol}(\mathbf{r}) \qquad (1)$$

Here, $w_A(\mathbf{r})$ is a weight function that distributes the molecular electron density $\rho_{mol}(\mathbf{r})$ among all constituting atoms. The weight function fulfills $\forall \mathbf{r} \in \mathbb{R}^3 : \sum_A w_A(\mathbf{r}) = 1$ to guarantee an exhaustive partitioning, i.e., $\sum_A \rho_A(\mathbf{r}) = \rho_{mol}(\mathbf{r})$. Real-space methods are either binary with $w_A(\mathbf{r}) \in \{0, 1\}$, like the quantum theory of atoms in molecules (QTAIM) [2–4] and Voronoi tessellation [5], or fuzzy with $w_A(\mathbf{r}) \in [0, 1]$, like the Becke [6], Politzer [7], and Hirshfeld family of partitioning [8–16; Heidar-Zadeh et al. 2017, (unpublished)] schemes. The Hirshfeld method [8] specifically requires a promolecular density $\rho_{mol}^0(\mathbf{r})$, which corresponds to the sum of reference proatom densities centered at the position of atomic nuclei,

$$\rho_{\text{mol}}^0(\mathbf{r}) = \sum_{\text{B}}^{N_{atoms}} \rho_{\text{B}}^0(\mathbf{r}) \tag{2}$$

The atomic weight function is then computed according to the stockholder recipe,

$$w_{\text{A}}(\mathbf{r}) = \frac{\rho_{\text{A}}^0(\mathbf{r})}{\rho_{\text{mol}}^0(\mathbf{r})}. \tag{3}$$

This implies that, at every point in space, the gain or loss in the electron density upon going from the promolecule to the molecular density is distributed among all atoms using their share in the promolecular density, i.e.,

$$\begin{aligned} \rho_{\text{A}}(\mathbf{r}) - \rho_{\text{A}}^0(\mathbf{r}) &= w_{\text{A}}(\mathbf{r}) \Delta\rho_{\text{mol}}(\mathbf{r}) \\ &= w_{\text{A}}(\mathbf{r})\left[\rho_{\text{mol}}(\mathbf{r}) - \rho_{\text{mol}}^0(\mathbf{r})\right] \end{aligned} \tag{4}$$

Inspired by Politzer's earlier work [7, 17–20], in 1977 Hirshfeld [8] used spherically-averaged isolated neutral proatom densities and introduced the stockholder partitioning weight in Eq. (3). The arbitrary choice of neutral proatom densities has been recognized as one of the major drawbacks of the Hirshfeld partitioning [9, 21, 22]. In addition, Hirshfeld charges are known to be very small in magnitude; this can be rationalized based on the fact that minimizing the sum of f-divergence measures between atomic and reference proatom densities uniquely yields Hirshfeld AIM densities for an exhaustive partitioning [23–29]. In other words, Hirshfeld AIM densities are variationally optimized to be as close as possible to the neutral reference proatom densities, so the Hirshfeld AIM are nearly neutral also.

The first, and still the most popular, approach to systematically select suitable proatom densities, called the iterative Hirshfeld method (Hirshfeld-I) [9, 30; Heidar-Zadeh et al. 2017, (unpublished)], was developed in 2007 by Bultinck *et al.* using a self-consistent algorithm, which defines the atomic density at i^{th} iteration through,

$$\rho_{\text{A}}^{(i)}(\mathbf{r}) = \left(\frac{\rho_{\text{A}}^0\left(\mathbf{r}, N_{\text{A}}^{(i-1)}\right)}{\sum_{\text{B}}\rho_{\text{B}}^0\left(\mathbf{r}, N_{\text{B}}^{(i-1)}\right)}\right)\rho_{\text{mol}}(\mathbf{r}) \tag{5}$$

where $N_{\text{A}}^{(i-1)}$ represents the number of electrons of atom A at the $(i\text{-}1)^{\text{th}}$ iteration,

$$N_{\text{A}}^{(i-1)} = \int\rho_{\text{A}}^{(i-1)}(\mathbf{r})d\mathbf{r}. \tag{6}$$

The reference proatom density with N_{A} electrons is defined as a weighted average of the atomic densities with the closest-lower-integer number, $\lfloor N_{\text{A}}\rfloor$, and the closest-higher-integer number, $\lceil N_{\text{A}}\rceil$, of electrons [31–34],

$$\begin{aligned} \rho_{\text{A}}^0(\mathbf{r}, N_{\text{A}}) &= (N_{\text{A}} - \lfloor N_{\text{A}}\rfloor)\rho_{\text{A}}^0(\mathbf{r}, \lceil N_{\text{A}}\rceil) \\ &\quad + (\lceil N_{\text{A}}\rceil - N_{\text{A}})\rho_{\text{A}}^0(\mathbf{r}, \lfloor N_{\text{A}}\rfloor). \end{aligned} \tag{7}$$

This iterative scheme conventionally uses Hirshfeld charges as initial guess, refines the atomic densities self-consistently, and converges when the change in AIM populations is sufficiently small, $\underset{\text{A}}{\max}\left|N_{\text{A}}^{(i)} - N_{\text{A}}^{(i-1)}\right| \leq \varepsilon$ with ε being a user-defined threshold. The popularity of the Hirshfeld-I charges can be attributed to their intuitive appeal, limited basis set dependence [30, 35, 36] and accurate modeling of the molecular electrostatic potential on molecular van der Waals' surfaces, even without including the contributions from the dipole or higher-order multipoles [37].

The major weakness of the Hirshfeld-I scheme is its dependence on the electron density of negatively-charged atomic species. Even when an atomic charge becomes only slightly negative during the self-consistent iterations, the interpolated density in Eq. (7) requires the corresponding anion density of proatom A with nuclear charge Z_{A}. Unfortunately, in some cases the extra electron(s) of the negatively charged atomic species (like the nitrogen anion or the dianion of all atoms) are not physically bound, even if they are computationally (i.e., basis-set) bound. It is also possible for the anion density to be physically bound, but computationally unbound (like the hydrogen and oxygen anions at the Hartree-Fock level of theory). This pitfall can easily go unnoticed, and induces, especially for large basis sets, a very slow decay of the negatively-charged atomic density. For example, the unbound oxygen dianion density is required for computing the charges of metal oxides, where the Hirshfeld-I charge is below −1. This results in an unreasonably negative atomic charge for the oxygen atom and poor approximations of the electrostatic potential on molecular van der Waals' surfaces. Also, the density of these unbound, or barely bound, reference atomic species heavily depends on the level of theory and basis set used, and can even exhibit non-monotonic decay [38].

Several, typically pragmatic, remedies have been proposed to address the "anion problem" in Hirshfeld-I, often at the expense of increased computational cost and/or defining "effective" atom densities in a way that is at best ad hoc and at worst hand-tuned [16, 39, 40]. Here, we introduce a simple yet novel technique to obtain physically-bound densities for negatively charged reference proatom species using fractional nuclear charges. These bound reference densities decay monotonically at a reasonable rate and alleviate the shortcomings of the Hirshfeld-I charges when applied to compounds containing negatively charged atoms.

Methods

Our approach for obtaining a bound anion density is based on the observation that one can bind the extra electron(s) by increasing the positive nuclear charge. Suppose that the Hirshfeld-I scheme requires the proatom

density of an element with atomic number Z_A and $N_A >$ Z_A electrons. One should first assess whether the N_A electrons are bound at the given level of theory and basis set by computing the electron affinity,

$$E(Z_A, N_A-1) - E(Z_A, N_A) \geq 0 \tag{8}$$

If this condition is met, N_A electrons are bound by the nuclear charge Z_A at the given level of theory, and the Hirshfeld-I procedure can be carried out in the conventional way, using the computed $\rho_A(\mathbf{r}, N_A; Z_A)$ density with integer atomic number Z_A. For some atomic anions and all dianion species, Eq. (8) is not satisfied and the densities have the undesirable features mentioned above. Therefore, we search for the lowest effective nuclear charge Z_A^{eff} that will effectively bind N_A electrons, i.e., the Z_A^{eff} that solves the following equation,

$$E(Z_A^{\text{eff}}, N_A) - E(Z_A^{\text{eff}}, N_A-1) = 0 \tag{9}$$

Though there is intrinsic interest in the value of Z_A^{eff} and the associated critical behavior [41–47], in this application we are interested mainly in the corresponding ground-state density of the system with N_A electrons, i.e., $\rho_A(\mathbf{r}, N_A; Z_A^{\text{eff}})$. Still, using this density directly is not desirable because it does not meet the nuclear cusp condition [48, 49]. So, we usually opt to transform it by coordinate scaling [50] to exhibit the cusp associated with a nuclear charge of Z_A (see Appendix),

$$\rho_A(\mathbf{r}, N_A; Z_A) = \left(\frac{Z_A}{Z_A^{\text{eff}}}\right)^3 \rho_A\left(\frac{Z_A}{Z_A^{\text{eff}}}\mathbf{r}, N_A; Z_A^{\text{eff}}\right). \tag{10}$$

This bound pseudo-density for the N_A-electron system can then be used in the Hirshfeld-I procedure.

Such critical nuclear charges have already been reported in the literature. For example, Hogreve [42] computed these values using multi reference configuration interaction methods with large and diffuse basis sets. Sergeev and Kais [44] reported these values by using a one-particle model to describe the motion of the loosely bound electron. Recently, Cardenas et al. [47] estimated these values using ionization-potential extrapolation of isoelectronic series. Even though these reported values seem like a good choice in the first place, our numerical tests revealed that Z_A^{eff} should be found at each level of theory and basis set to keep the electrons bound. This is especially important, because it is commonly advised to use the same level of theory and basis set for molecular and proatom density calculations.

In practice, for a given level of theory and basis set, Z_A^{eff} in Eq. (9) can be solved for using Newton's method considering the fact that the derivative of the energy

with respect to the atomic number Z_A is the electrostatic potential at the position of the nucleus A [51–57],

$$\frac{\partial E}{\partial Z_A} = \Phi(\mathbf{r} = \mathbf{R}_A) = -\int \frac{\rho(\mathbf{r}')}{|\mathbf{r}' - \mathbf{R}_A|} d\mathbf{r}'. \tag{11}$$

In other words, the atomic number can be iteratively updated until convergence is reached according to,

$$\xi_A^{(k+1)} = \xi_A^{(k)} - \frac{E\left(N_A-1, \xi_A^{(k)}\right) - E\left(N_A, \xi_A^{(k)}\right)}{\Phi\left(\mathbf{r} = \mathbf{R}_A, N_A-1, \xi_A^{(k)}\right) - \Phi\left(\mathbf{r} = \mathbf{R}_A, N_A, \xi_A^{(k)}\right)} \tag{12}$$

Alternatively, for a given level of theory and basis set, one can define the effective nuclear charge as the smallest nuclear charge for which the energy of the highest molecular orbital becomes negative to guarantee that all N_A electrons are bound.

$$E_{\text{HOMO}}(N_A, Z_A^{\text{eff}}) \leq 0 \tag{13}$$

This can be found by scanning the nuclear charge in a reasonable interval like $[N_A - 1, N_A]$.

Results and discussion

To demonstrate how the atomic densities corresponding to the effective nuclear charges can remove the artifacts associated with unbound anionic proatom densities, we closely examine Hirshfeld-I charges of ammonia and formamide. We focused on molecules containing the nitrogen atom because such molecules are typically the most problematic for Hirshfeld-I caused by the fact that the nitrogen is relatively electronegative, so the nitrogen AIM has typically a negative charge, but the isolated nitrogen atom has no bound anion. (Indeed, the Hirshfeld-I charges of nitrogen AIM can become absurdly negative. For example, the charge of the nitrogen atom in NLi_3 is *less than minus three* when diffuse basis functions are used!)

All geometries were optimized at $U\omega B97XD$/cc-pVTZ level of theory, followed by single point calculations using unrestricted Hartree-Fock and the UB3LYP [58, 59] and $U\omega B97XD$ [60] density functionals in conjunction with 12 Dunning (d-aug-)cc-pVXZ with X = D, T, Q, 5 correlation consistent basis sets [61]. All quantum chemistry calculations were performed using *Gaussian09* [62], employing ultrafine integration grids and the stable = opt keyword to ensure that a (local) minimum of the energy with respect to variations of the orbitals was found. The Hirshfeld-I calculations were performed with the HORTON [63] and ChemTools [64] packages. The finest pruned Becke-Lebedevgrid of HORTON has been used to compute the molecular density, and exponential radial grids extending from 0.0005 to 20 Angstrom with 175

radial and 230 angular Lebedev-Laikov grid points are used to represent the proatom densities.

Table 1 presents the optimized effective nuclear charges for the anion and dianion species of the carbon, nitrogen, and oxygen atoms at various levels of theory using Eq. (12); these critical charges obtained by having zero electron affinity are labeled as ECR (energy-determined critical charges). In addition, the smallest effective nuclear charges satisfying Eq. (13) are also tabulated for the nitrogen anion and dianion; these critical charges obtained by having zero HOMO energy are labeled as HCR (HOMO-determined critical charges). The

original basis set of each element has been used for the computations of atoms with fractional nuclear charge. We also scaled the basis set exponents of each atom by $\sqrt{\frac{Z_A^{eff}}{Z_A}}$, but found that this barely changed the final Z_A^{eff} values. It is important to note that even the oxygen anion, which is physically bound, is slightly unbound at Hartree-Fock level of theory (especially when using small basis sets). On the other hand, if $Z_A^{eff} < Z_A$ for binding N_A electrons, we use the original nuclear charge Z_A and the accompanying density $\rho_A(\mathbf{r}, N_A; Z_A)$ as reference proatom density in Hirshfeld-I computation. That is, the

Table 1 Effective nuclear charges computed from Eqs. (12) and (13), called Z_{ECR} and Z_{HCR}, for the anion and dianion of carbon, nitrogen, and oxygen at different levels of theory. Data for species that are unbound for Z_A and hence have a larger effective nuclear charge than Z_A are shown in bold

Level of theory	Z_{ECR} from Eq. (12)						Z_{HCR} from Eq. (13)	
	C^-	N^-	O^-	C^{-2}	N^{-2}	O^{-2}	N^-	N^{-2}
UHF/cc-pVDZ	**6.02**	**7.24**	**8.12**	**7.17**	**8.08**	**8.97**	7.13	7.94
UHF/cc-pVTZ	5.99	**7.21**	**8.09**	**7.18**	**8.06**	**8.93**	7.07	7.87
UHF/cc-pVQZ	5.97	**7.20**	**8.07**	**7.18**	**8.06**	**8.93**	7.04	7.86
UHF/cc-pV5Z	5.96	**7.19**	**8.05**	**7.18**	**8.05**	**8.92**	7.03	7.83
UHF/aug-cc-pVDZ	5.95	**7.18**	**8.04**	**7.14**	**8.02**	**8.90**	7.07	7.82
UHF/aug-cc-pVTZ	5.95	**7.18**	**8.05**	**7.18**	**8.04**	**8.91**	7.08	7.83
UHF/aug-cc-pVQZ	5.95	**7.18**	**8.05**	**7.18**	**8.05**	**8.92**	7.08	7.83
UHF/aug-cc-pV5Z	5.95	**7.18**	**8.05**	**7.18**	**8.05**	**8.92**	7.10	7.83
UHF/d-aug-cc-pVDZ	5.95	**7.18**	**8.04**	**7.14**	**8.02**	**8.90**	7.16	7.83
UHF/d-aug-cc-pVTZ	5.95	**7.18**	**8.05**	**7.18**	**8.04**	**8.91**	7.15	7.85
UHF/d-aug-cc-pVQZ	5.95	**7.18**	**8.05**	**7.18**	**8.05**	**8.92**	7.15	7.85
UHF/d-aug-cc-pV5Z	5.95	**7.18**	**8.05**	**7.18**	**8.05**	**8.92**	7.15	7.85
UB3LYP/cc-pVDZ	5.97	**7.13**	**8.03**	**7.04**	**7.98**	**8.88**	7.44	8.28
UB3LYP/cc-pVTZ	5.93	**7.06**	7.96	**7.01**	**7.91**	**8.80**	7.36	8.20
UB3LYP/cc-pVQZ	5.90	**7.04**	7.92	**7.00**	**7.90**	**8.78**	7.33	8.19
UB3LYP/cc-pV5Z	5.87	**7.01**	7.89	**6.99**	**7.87**	**8.75**	7.30	8.16
UB3LYP/aug-cc-pVDZ	5.84	6.98	7.85	**6.96**	**7.84**	**8.72**	7.28	8.12
UB3LYP/aug-cc-pVTZ	5.84	6.98	7.85	**6.97**	**7.85**	**8.72**	7.27	8.13
UB3LYP/aug-cc-pVQZ	5.84	6.98	7.85	**6.97**	**7.85**	**8.72**	7.27	8.13
UB3LYP/aug-cc-pV5Z	5.84	6.97	7.85	**6.97**	**7.85**	**8.72**	7.27	8.13
UB3LYP/d-aug-cc-pVDZ	5.83	6.96	7.84	**6.93**	**7.84**	**8.71**	7.28	8.12
UB3LYP/d-aug-cc-pVTZ	5.83	6.95	7.84	**6.94**	**7.84**	**8.72**	7.27	8.13
UB3LYP/d-aug-cc-pVQZ	5.83	6.95	7.84	**6.94**	**7.84**	**8.72**	7.27	8.13
UB3LYP/d-aug-cc-pV5Z	5.83	6.95	7.84	**6.94**	**7.84**	**8.72**	7.27	8.13
UωB97XD/cc-pVDZ	5.96	**7.13**	**8.03**	**7.06**	**7.98**	**8.88**	7.27	8.13
UωB97XD/cc-pVTZ	5.93	**7.08**	7.97	**7.03**	**7.92**	**8.80**	7.19	8.02
UωB97XD/cc-pVQZ	5.90	**7.06**	7.93	**7.03**	**7.91**	**8.79**	7.15	8.00
UωB97XD/cc-pV5Z	5.88	**7.03**	7.90	**7.02**	**7.89**	**8.76**	7.11	7.96
UωB97XD/aug-cc-pVDZ	5.85	**7.01**	7.87	**6.99**	**7.86**	**8.73**	7.06	7.90
UωB97XD/aug-cc-pVTZ	5.85	**7.01**	7.87	**7.00**	**7.87**	**8.74**	7.06	7.91
UωB97XD/aug-cc-pVQZ	5.85	**7.01**	7.87	**7.01**	**7.87**	**8.74**	7.05	7.91
UωB97XD/aug-cc-pV5Z	5.85	**7.01**	7.87	**7.01**	**7.87**	**8.74**	7.05	7.90
UωB97XD/d-aug-cc-pVDZ	5.84	7.00	7.86	**6.99**	**7.86**	**8.73**	7.05	7.89
UωB97XD/d-aug-cc-pVTZ	5.85	7.00	7.87	**6.99**	**7.86**	**8.73**	7.05	7.89
UωB97XD/d-aug-cc-pVQZ	5.85	7.00	7.87	**7.00**	**7.87**	**8.74**	7.05	7.89
UωB97XD/d-aug-cc-pV5Z	5.85	7.00	7.87	**7.00**	**7.87**	**8.74**	7.05	7.89

density corresponding to the critical atomic number is not used when the conventional Hirshfeld-I proatoms are already bound.

The densities corresponding to critical atomic charges tabulated in Table 1 have been used to compute the atomic charges of NH_3 in Fig. 1. This example highlights the large spread of Hirshfeld-I charges when the commonly used unbound anionic proatom densities are used. In such cases, the decay of the nitrogen anion density depends very strongly on the level of theory and basis set used, directly affecting the decay of the nitrogen AIM density and its charge. The very diffuse proatom densities for the nitrogen anion cause the nitrogen to "steal" extra electrons from its neighbouring atoms, and when its charge decreases below −1 then the nitrogen dianion density must also be included for the algorithm to converge. This "runaway charge" problem and other artifacts caused by using unphysical proatom densities are greatly reduced by using the more realistic densities corresponding to the effective nuclear charges obtained through Eqs. (12) and (13). These densities are either scaled according to Eq. (10) or not, which has a noticeable influence on the magnitude (but not the spread) of the nitrogen AIM charges. The suffix -S is used to denote that the

(di)anion densities are scaled before being used as reference proatom densities in the Hirshfeld-I algorithm.
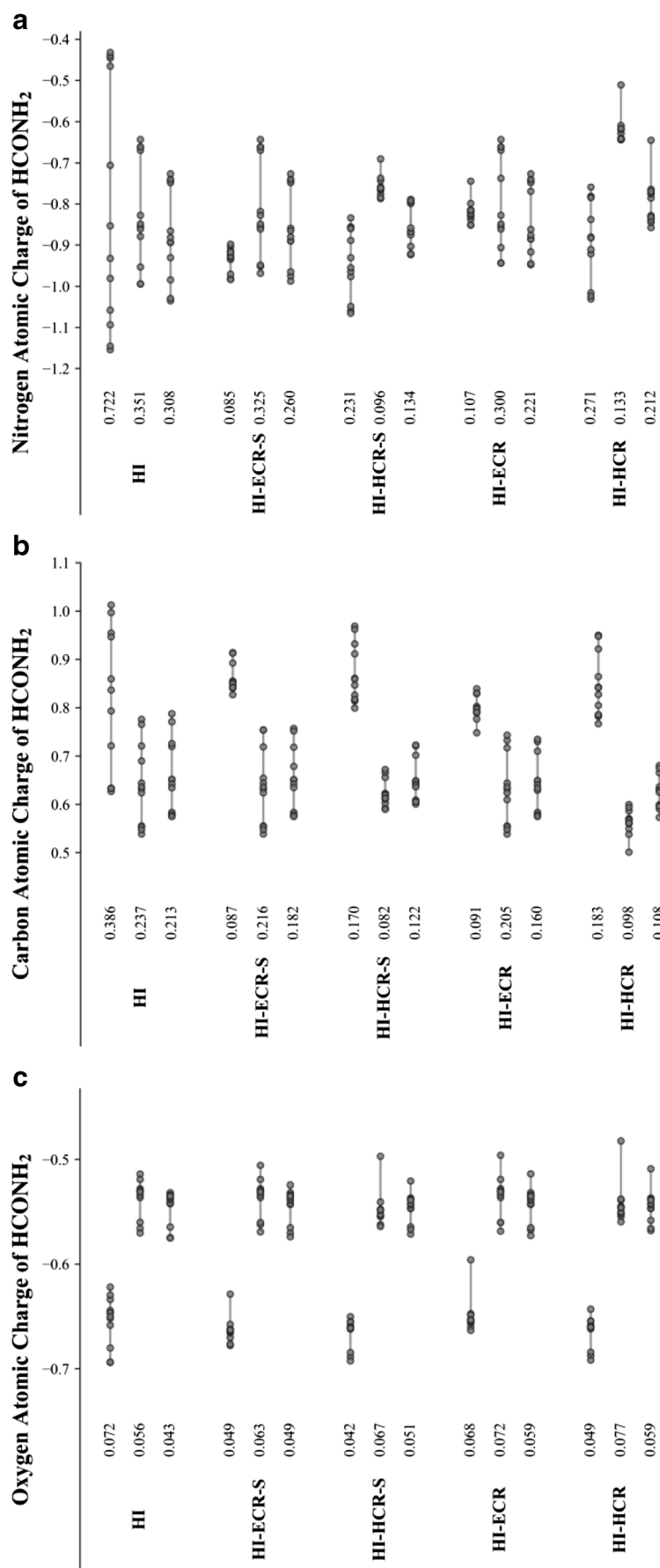
From nitrogen charges computed with the effective nuclear charges obtained through Eq. (12), i.e., HI-ECR and HI-ECR-S, it is immediately clear that this treatment works very well at the Hartee-Fock level of theory, where the nitrogen anion is unbound for all basis sets considered, $Z_A^{eff} > 7$. These Hartee-Fock charges have a small spread and a reasonable negative value larger than −1, so our treatment eliminates the need for nitrogen dianion density. The effect on the charges computed with density functional theory (DFT) is less pronounced, because the UB3LYP/(d-)aug-cc-pVXZ and UωB97XD/d-aug-cc-pVXZ methods fictitiously recognize the nitrogen anion as bound with $Z_A^{eff} < 7$. However, the charges computed with UB3LYP/cc-pVXZ and UωB97XD/(aug-)cc-pVXZ slightly change because the nitrogen anion is slightly unbound with those methods. For nitrogen charges computed with effective nuclear charges obtained through Eq. (13), i.e., HI-HCR and HI-HCR-S, the nitrogen anion has $Z_A^{eff} > 7$ at all levels of theory and basis sets, so the nitrogen anion density is replaced at all levels of theory and basis sets considered. The Hartree-Fock charges are more spread than HI-ECR and HI-ECR-S, because the effective nuclear charges obtained are smaller. However, the DFT charges have a smaller spread when
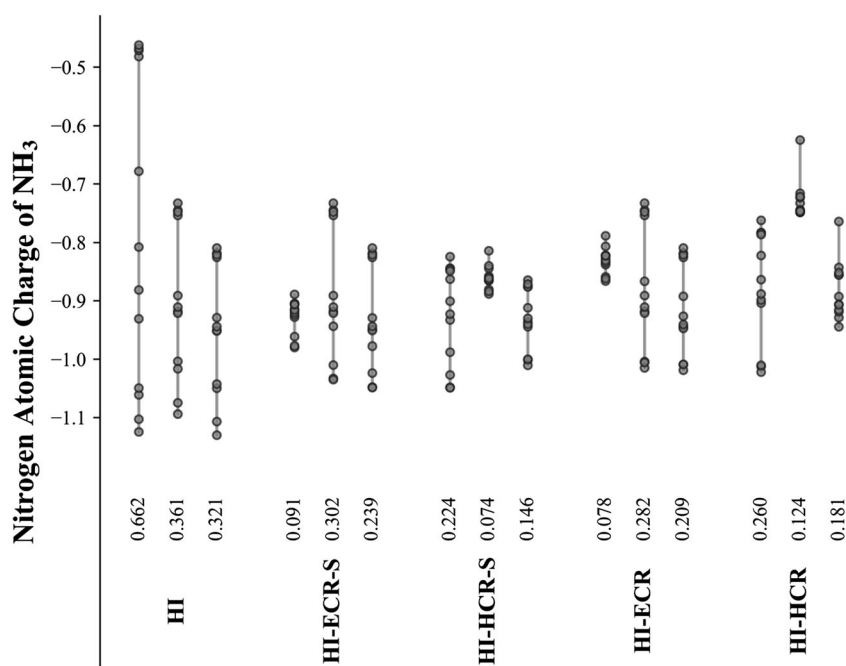
Fig. 1 Ammonia AIM charges from the original iterative Hirshfeld (HI) scheme and those computed using the critical nuclear charge proatoms for nitrogen. The charges computed using the fractional nuclear charge approach are labeled HI-ECR-S and HI-HCR-S for which the effective nuclear charge of the nitrogen anion has been computed using Eqs. (12) and (13), respectively, and the corresponding density is scaled according to Eq. (10). The same procedures, without scaling the density, have been used to compute HI-ECR and HI-HCR charges. For each scheme, the three

columns correspond to UHF, UB3LYP, and UωB97XD levels of theory, respectively, and each column shows the charges computed using 12 Dunning basis sets: cc-pVXZ, aug-cc-pVXZ, and d-aug-cc-pVXZ with X = D, T, Q, 5. The molecular and proatom densities were computed at the same level of theory. The absolute range of the atomic charges obtained using various basis sets for each level of theory is summarized on the *x*-axis alongside the partitioning method. The actual charges are tabulated in Table S1 of the Supplementary material

a

Nitrogen Atomic Charge of HCONH$_2$

0.722   0.351   0.308   0.085   0.325   0.260   0.231   0.096   0.134   0.107   0.300   0.221   0.271   0.133   0.212

HI   **HI-ECR-S**   **HI-HCR-S**   **HI-ECR**   **HI-HCR**

b

Carbon Atomic Charge of HCONH$_2$

0.386   0.237   0.213   0.087   0.216   0.182   0.170   0.082   0.122   0.091   0.205   0.160   0.183   0.098   0.108

HI   **HI-ECR-S**   **HI-HCR-S**   **HI-ECR**   **HI-HCR**

c

Oxygen Atomic Charge of HCONH$_2$

0.072   0.056   0.043   0.049   0.063   0.049   0.042   0.067   0.051   0.068   0.072   0.059   0.049   0.077   0.059

HI   **HI-ECR-S**   **HI-HCR-S**   **HI-ECR**   **HI-HCR**

◀ **Fig. 2** Formamide AIM charges from the original iterative Hirshfeld (HI) charges and those computed using the critical nuclear charge proatoms for a) nitrogen, b) carbon, and c) oxygen. The charges computed using the fractional nuclear charge approach are labeled HI-ECR-S and HI-HCR-S for which the effective nuclear charges of the anions have been computed using Eqs. (12) and (13), respectively, and the corresponding density is scaled according to Eq. (10). The same procedures, without scaling the density, have been used to compute HI-ECR and HI-HCR charges. For each scheme, the three columns correspond to UHF, UB3LYP, and UωB97XD levels of theory, respectively, and each column shows the charges computed using 12 Dunning basis sets: cc-pVXZ, aug-cc-pVXZ, and d-aug-cc-pVXZ with X = D, T, Q, 5. The molecular and proatom densities were computed at the same level of theory. The absolute range of the atomic charges obtained using various basis sets for each level of theory is summarized on the x-axis alongside the partitioning method. The actual charges are tabulated in Table S2-S4 of the Supplementary material

compared to the HI-ECR and HI-ECR-S charges, because the anion densities are replaced with the corresponding density of Z_A^{eff} at all levels of theory.

Figure 2 shows the Hirshfeld-I charges of the carbon, nitrogen, and oxygen atoms of formamide at different levels of theory using the original and effective nuclear bound (di)anion proatom densities. The original Hirshfeld-I charges of carbon and nitrogen display a noticeable dependence on the basis set used. This dependence is removed when the nitrogen anion density is replaced with the density corresponding to the effective nuclear charge to yield a bound anionic system. Similar to NH_3, the charges are most affected at the Hartree-Fock level for HI-ECR and HI-ECR-S, and at the DFT level for HI-HCR and HI-HCR-S. We believe that the effective nuclear charges computed through Eq. (12) are more suitable, as they fully comply with ionization potential computations at each level of theory and basis set. For example, the nitrogen anion has a positive ionization potential at the UB3LYP/(d-)aug-cc-pVXZ and UωB97XD/d-aug-cc-pVXZ levels, implying that the electrons are bound, and the effective nuclear charge of the nitrogen atom for binding 8 electrons at these levels are less than 7 according to Eq. (12), but not based on Eq. (13). Consequently, we believe that the effective nuclear charges that yield a zero electron affinity for binding the extra electron(s) at each level of theory and basis set, Z_{ECR}, are worth further investigation for (di)anion proatom species in the Hirshfeld-I algorithm.

Conclusions

The iterative Hirshfeld scheme is one of the most popular recent density partitioning schemes commonly used for identifying atoms in molecules and materials. The elegant self-consistent algorithm of Hirshfeld-I is known to converge almost always to a unique solution and is almost insensitive to the choice of initial proatoms. However, very often, Hirshfeld-

I calculations require the proatom densities from unbound isolated atomic anions and/or dianions. Conventionally one (often with great difficulty) determines the (only basis-set-bound) densities of these ions with the same electronic structure method and basis set as the molecular calculation. However, this often leads to Hirshfeld-I charges that are too large in magnitude and too sensitive to the level of theory and basis set used for computing the molecular and reference proatom densities. Here we proposed a novel approach to obtain reasonable densities for unbound (di)anion atomic species. The key idea is based on exploiting the densities corresponding to the effective nuclear charges, i.e., the smallest atomic number Z_A^{eff} for which N_A electrons are bound. This requires computing the critical atomic number of unbound atomic species at a given level of theory and basis set, and utilizing the corresponding scaled bound density as a reference density. Our result shows that this protocol produces reasonably decaying atomic densities and improves the computational robustness of Hirshfeld-I algorithm.

As an alternative, one can also use a fixed level of theory and basis set to compute the reference proatom densities. This considerably reduces the spread of Hirshfeld-I charges and makes them insensitive to the level of theory and basis set used for the molecule or material being partitioned, though a suitable definition for the electron density of unbound atomic anions and polyanions is still required. Currently, we are constructing an accurate database of ground and excited state densities of neutral and charged atomic species using multi-reference configuration interaction methods with large basis sets. We believe that combining the critical-charge and density scaling approach in this paper with the high-quality densities from this database will guarantee the computational robustness of Hirshfeld-I.

Appendix

Here we demonstrate how density is scaled to have the right cusp according to Eq. (10). The exact cusp relation for the N_A-electron ground-state electron density of an atom with charge Z_A^{eff} is

$$-2Z_A^{\text{eff}} = \left[\frac{1}{\rho_A\left(r,\theta,\phi;N_A;Z_A^{\text{eff}}\right)} \frac{\partial\rho_A\left(r,\theta,\phi;N_A;Z_A^{\text{eff}}\right)}{\partial r} \right]_{r=0}$$

$$(14)$$

Scaling the density according to Eq. (10) fixes the cusp condition,

$$\left[\frac{1}{\left(\frac{Z_A}{Z_A^{\text{eff}}}\right)^3 \rho_A\left(\frac{Z_A}{Z_A^{\text{eff}}}r,\theta,\phi,N_A;Z_A^{\text{eff}}\right)} \frac{\partial\left(\frac{Z_A}{Z_A^{\text{eff}}}\right)^3 \rho_A\left(\frac{Z_A}{Z_A^{\text{eff}}}r,\theta,\phi,N_A;Z_A^{\text{eff}}\right)}{\partial r} \right]_{r=0}$$

$$= -2Z_A^{\text{eff}}\left(\frac{Z_A}{Z_A^{\text{eff}}}\right)$$

$$= -2Z_A$$

$$(15)$$

while maintaining the normalization of the electron density, i.e.,

$$\int_{-\infty}^{\infty}\int_{-\infty}^{\infty}\int_{-\infty}^{\infty}\left(\frac{Z_A}{Z_A^{\text{eff}}}\right)^3 \rho_A\left(\frac{Z_A}{Z_A^{\text{eff}}}x,\frac{Z_A}{Z_A^{\text{eff}}}y,\frac{Z_A}{Z_A^{\text{eff}}}z,N_A;Z_A^{\text{eff}}\right)dxdydz$$

$$= \int_{-\infty}^{\infty}\int_{-\infty}^{\infty}\int_{-\infty}^{\infty}\rho_A\left(\frac{Z_A}{Z_A^{\text{eff}}}x,\frac{Z_A}{Z_A^{\text{eff}}}y,\frac{Z_A}{Z_A^{\text{eff}}}z,N_A;Z_A^{\text{eff}}\right)d\left(\frac{Z_A}{Z_A^{\text{eff}}}x\right)d\left(\frac{Z_A}{Z_A^{\text{eff}}}y\right)d\left(\frac{Z_A}{Z_A^{\text{eff}}}z\right).$$

$$= \int_{-\infty}^{\infty}\int_{-\infty}^{\infty}\int_{-\infty}^{\infty}\rho_A\left(X,Y,Z,N_A;Z_A^{\text{eff}}\right)dXdYdZ$$

$$= N_A$$

$$(16)$$

References

1. Bultinck P, Popelier PLA (2009) Atoms in molecules and population analysis. In: Chattaraj PK (Ed) Theory of chemical reactivity. Taylor and Francis, London, pp 215–227
2. Bader RFW (1990) Atoms in molecules: a quantum theory. Clarendon, Oxford
3. Heidarzadeh F, Shahbazian S (2011) The quantum divided basins: a new class of quantum subsystems. Int J Quantum Chem 111(12): 2788–2801
4. Zadeh FH, Shahbazian S (2010) Toward a fuzzy atom view within the context of the quantum theory of atoms in molecules: quasi-atoms. Theor Chem Accounts 128(2):175–181
5. Okabe A, Boots B, Sugihara K, Chiu SN, Kendall DG (2008) Spatial tessellations: concepts and applications of voronoi diagrams. In: Spatial tessellations, second edn. Wiley, New York
6. Becke AD (1988) A multicenter numerical integration scheme for polyatomic molecules. J Chem Phys 88(4):2547–2553
7. Politzer P, Harris RR (1970) Electronic density distribution in nitric oxide. J Am Chem Soc 92(7):1834–1836
8. Hirshfeld FL (1977) Bonded-atom fragments for describing molecular charge densities. Theor Chim Acta 44(2):129–138
9. Bultinck P, Van Alsenoy C, Ayers PW, Carbo-Dorca R (2007) Critical analysis and extension of the Hirshfeld atoms in molecules. J Chem Phys 126(14):144111
10. Verstraelen T, Vandenbrande S, Heidar-Zadeh F, Vanduyfhuys L, Van Speybroeck V, Waroquier M, Ayers PW (2016) Minimal basis iterative stockholder: atoms in molecules for force-field development. J Chem Theory Comput 12(8):3894–3912
11. Geldof D, Krishtal A, Blockhuys F, Van Alsenoy C (2011) An extension of the Hirshfeld method to open Shell systems using fractional occupations. J Chem Theory Comput 7(5):1328–1335
12. Ghillemijn D, Bultinck P, Van Neck D, Ayers PW (2011) A self-consistent Hirshfeld method for the atom in the molecule based on minimization of information loss. J Comput Chem 32(8):1561–1567
13. Verstraelen T, Ayers PW, Van Speybroeck V, Waroquier M (2013) Hirshfeld-E partitioning: AIM charges with an improved trade-off between robustness and accurate electrostatics. J Chem Theory Comput 9(5):2221–2225
14. Lillestolen TC, Wheatley RJ (2008) Redefining the atom: atomic charge densities produced by an iterative stockholder approach. Chem Commun 45:5909
15. Verstraelen T, Ayers PW, Van Speybroeck V, Waroquier M (2012) The conformational sensitivity of iterative stockholder partitioning schemes. Chem Phys Lett 545:138–143
16. Manz TA, Limas NG (2016) Introducing DDEC6 atomic population analysis: part 1. Charge partitioning theory and methodology. RSC Adv 6(53):47771–47801
17. Politzer P (1970) Atom promotion and bond properties in the hydrogen and the lithium molecules. Theor Chim Acta 16(2):120–125
18. Politzer P, Leung KC, Elliott JD, Peters SK (1975) Properties of atoms in molecules. Theor Chim Acta 38(2):101–107
19. Politzer P, Reggio PH (1972) Properties of atoms in molecules. IV. Atomic charges in some linear polyatomic molecules. J Am Chem Soc 94(24):8308–8311
20. Politzer P (1971) Properties of atoms in molecules. Theor Chim Acta 23(2):203–207
21. Francisco E, Pendas AM, Blanco MA, Costales A (2007) Comparison of direct and flow integration based charge density population analyses. J Phys Chem A 111(48):12146–12151
22. Davidson ER, Chakravorty S (1992) A test of the Hirshfeld definition of atomic charges and moments. Theor Chim Acta 83(5–6): 319–330
23. Nalewajski RF, Parr RG (2001) Information theory thermodynamics of molecules and their Hirshfeld fragments. J Phys Chem A 105(31):7391–7400
24. Nalewajski RF, Parr RG (2000) Information theory, atoms in molecules, and molecular similarity. Proc Natl Acad Sci 97(16):8879–8882
25. Ayers PW (2000) Atoms in molecules, an axiomatic approach. I. Maximum transferability. J Chem Phys 113(24):10886–10898
26. Heidar-Zadeh F, Ayers PW (2015) How pervasive is the Hirshfeld partitioning? J Chem Phys 142(4):044107
27. Heidar-Zadeh F, Ayers PW, Bultinck P (2014) Deriving the Hirshfeld partitioning using distance metrics. J Chem Phys 141(9)"094103
28. Heidar-Zadeh F, Vinogradov I, Ayers PW (2017) Hirshfeld partitioning from non-extensive entropies. Theor Chem Accounts 136(4):54
29. Heidar-Zadeh F, Ayers PW (2017) Fuzzy atoms in molecules from Bregman divergences. Theor Chem Accounts 136(8):92
30. Bultinck P, Ayers PW, Fias S, Tiels K, Van Alsenoy C (2007) Uniqueness and basis set dependence of iterative Hirshfeld charges. Chem Phys Lett 444(1–3):205–208
31. Perdew JP, Parr RG, Levy M, Balduz JL (1982) Density-functional theory for fractional particle number: derivative discontinuities of the energy. Phys Rev Lett 49(23):1691–1694
32. Yang W, Zhang Y, Ayers PW (2000) Degenerate ground states and a fractional number of electrons in density and reduced density matrix functional theory. Phys Rev Lett 84(22):5172–5175
33. Ayers PW (2008) The continuity of the energy and other molecular properties with respect to the number of electrons. J Math Chem 43: 285–303
34. Ayers PW, Levy M (2000) Perspective on "density functional approach to the frontier-electron theory of chemical reactivity" by Parr RG, Yang W (1984). Theor Chem Accounts 103:353–360

35. Verstraelen T, Van Speybroeck V, Waroquier M (2009) The electronegativity equalization method and the split charge equilibration applied to organic systems: parametrization, validation, and comparison. J Chem Phys 131(4):044127

36. Verstraelen T, Pauwels E, De Proft F, Van Speybroeck V, Geerlings P, Waroquier M (2012) Assessment of atomic charge models for gas-phase computations on polypeptides. J Chem Theory Comput. 8(2):661–676

37. Van Damme S, Bultinck P, Fias S (2009) Electrostatic potentials from self-consistent Hirshfeld atomic charges. J Chem Theory Comput 5(2):334–340

38. Weinstein H, Politzer P, Srebrenik S (1975) A misconception concerning the electronic density distribution of an atom. Theor Chim Acta 38(2):159–163

39. Limas NG, Manz TA (2016) Introducing DDEC6 atomic population analysis: part 2. Computed results for a wide range of periodic and nonperiodic materials. RSC Adv 6(51):45727–45747

40. Vanpoucke DEP, Bultinck P, Cottenier S, Van Speybroeck V, Van Driessche I (2011) DFT study of La2Ce2O7: distorted fluorite versus pyrochlore structure. Phys Rev B 84:054110

41. Chakravorty SJ, Davidson ER (1996) Refinement of the asymptotic Z expansion for the ground-state correlation energies of atomic ions. J Phys Chem 100(15):6167–6172

42. Hogreve H (1998) On the maximal electronic charge bound by atomic nuclei. J Phys B:At Mol Opt Phys 31:L439–L446

43. Hogreve H (1998) Destabilization of atomic anions: the case of F- and O2. Phys Scr 58(1):25

44. Sergeev AV, Kais S (1999) Critical nuclear charges for N-electron atoms. Int J Quantum Chem 75(4–5):533–542

45. Kais S, Serra P (2000) Quantum critical phenomena and stability of atomic and molecular ions. Int Rev Phys Chem 19(1):97–121

46. Kais S, Serra P (2003) Finite-size scaling for atomic and molecular systems. Adv Chem Phys 125:1–99

47. Cárdenas C, Heidar-Zadeh F, Ayers PW (2016) Benchmark values of chemical potential and chemical hardness for atoms and atomic ions (including unstable anions) from the energies of isoelectronic series. Phys Chem Chem Phys 18(36):25721–25734

48. Kato T (1957) On the eigenfunctions of many-particle systems in quantum mechanics. Commun Pure Appl Math 10(2):151–177

49. Steiner E (1963) Charge Densities in Atoms. J Chem Phys 39(9): 2365–2366

50. Levy M, Perdew JP (1985) Hellmann-Feynman, virial, and scaling requisites for the exact universal density functionals. Shape of the correlation potential and diamagnetic susceptibility for atoms. Phys Rev A 32(4):2010–2021

51. Wilson Jr EB (1962) Four-dimensional electron density function. J Chem Phys 36(8):2232–2233

52. Politzer P, Lane P, Concha MC (2002) Atomic and molecular energies in terms of electrostatic potentials at nuclei. Int J Quantum Chem 90(1):459–463

53. Politzer P, Jalbout AF, Jin P (2003) Some approximate atomic and molecular energy formulas. Collect Czechoslov Chem Commun 68(1):61–74

54. Politzer P (2004) Atomic and molecular energies as functionals of the electrostatic potential. Theor Chem Accounts 111(2):395–399

55. Amovilli C, March NH (2017) Variational quantum Monte Carlo results for N2, N2+ and C2– utilising the four-dimensional density of bright Wilson. Phys Chem Liq 55(3):281–290

56. Politzer P, Levy M (1987) Energy differences from electrostatic potentials at nuclei. J Chem Phys 87(8):5044–5046

57. Politzer P (1988) Correction. J Chem Phys 89(4):2590–2590

58. Becke AD (1988) Density-functional exchange-energy approximation with correct asymptotic behavior. Phys Rev A 38(6):3098–3100

59. Lee C, Yang W, Parr RG (1988) Development of the Colle-Salvetti correlation-energy formula into a functional of the electron density. Phys Rev B 37(2):785–789

60. Chai J-D, Head-Gordon M (2008) Long-range corrected hybrid density functionals with damped atom–atom dispersion corrections. PCCP 10(44):6615

61. Dunning TH (1989) Gaussian-basis sets for use in correlated molecular calculations. 1. The atoms boron through neon and hydrogen. J Chem Phys 90:1007–1023

62. Frisch MJ, Trucks GW, Schlegel HB et al.(2009) Gaussian 09 revision C.01. Gaussian Inc., Wallingford CT

63. Verstraelen T, Tecmer P, Heidar-Zadeh F, Boguslawski K, Chan M, Zhao Y, Kim TD, Vandenbrande S, Yang D, González-Espinoza GE, Fias S, Limacher PA, Berrocal D, Malek A, Ayers PW (2015) HORTON 2.0.0. http://theochem.github.com/horton/

64. Heidar-Zadeh F, Richer M, Fias S, Miranda-Quintana RA, Chan M, Franco-Perez M, Gonzalez-Espinoza CE, Kim TD, Lanssens C, Patel AHG, Yang XD, Vohringer-Martinez E, Cardenas C, Verstraelen T, Ayers PW (2016) An explicit approach to conceptual density functional theory descriptors of arbitrary order. Chem Phys Lett 660:307–312